


The intramembrane proteases SPPL2a and SPPL2b regulate the homeostasis of selected SNARE proteins

Moritz Ballin^{1,2}, Wolfram Griep^{1,2}, Mehul Patel², Martin Karl², Torben Mentrup², Jhon Rivera-Monroy³, Brian Foo³, Blanche Schwappach³ and Bernd Schröder² 

¹ Biochemical Institute, Christian Albrechts University Kiel, Kiel, Germany

² Institute of Physiological Chemistry, Technische Universität Dresden, Dresden, Germany

³ Department of Molecular Biology, University Medical Center Göttingen, Göttingen, Germany

Keywords

intramembrane proteolysis; membrane trafficking; protein degradation; signal peptide peptidase-like proteases; SNARE protein

Correspondence

B. Schröder, Institute for Physiological Chemistry, Medizinisch-Theoretisches Zentrum MTZ, Technische Universität Dresden, Fiedlerstraße 42, D-01307 Dresden, Germany
 Tel: +49 (0) 351 458 6450
 E-mail: bernd.schroeder@tu-dresden.de

Moritz Ballin and Wolfram Griep contributed equally to this article

(Received 15 March 2022, revised 28 June 2022, accepted 30 August 2022)

doi:10.1111/febs.16610

Signal peptide peptidase (SPP) and SPP-like (SPPL) aspartyl intramembrane proteases are known to contribute to sequential processing of type II-oriented membrane proteins referred to as regulated intramembrane proteolysis. The ER-resident family members SPP and SPPL2c were shown to also cleave tail-anchored proteins, including selected SNARE (soluble *N*-ethylmaleimide-sensitive factor attachment protein receptor) proteins facilitating membrane fusion events. Here, we analysed whether the related SPPL2a and SPPL2b proteases, which localise to the endocytic or late secretory pathway, are also able to process SNARE proteins. Therefore, we screened 18 SNARE proteins for cleavage by SPPL2a and SPPL2b based on cellular co-expression assays, of which the proteins VAMP1, VAMP2, VAMP3 and VAMP4 were processed by SPPL2a/b demonstrating the capability of these two proteases to proteolyse tail-anchored proteins. Cleavage of the four SNARE proteins was scrutinised at the endogenous level upon SPPL2a/b inhibition in different cell lines as well as by analysing VAMP1-4 levels in tissues and primary cells of SPPL2a/b double-deficient (dKO) mice. Loss of SPPL2a/b activity resulted in an accumulation of VAMP1-4 in a cell type- and tissue-dependent manner, identifying these proteins as SPPL2a/b substrates validated *in vivo*. Therefore, we propose that SPPL2a/b control cellular levels of VAMP1-4 by initiating the degradation of these proteins, which might impact cellular trafficking.

Introduction

Signal peptide peptidase (SPP) and the homologous SPP-like proteases SPPL2a, SPPL2b, SPPL2c and SPPL3 are GxGD-type aspartyl intramembrane proteases [1,2]. Similar to the enzymatically related presenilins as part of the γ -secretase complex, they possess the capability to cleave single-span transmembrane

substrate proteins within their transmembrane segment. Different family members exhibit divergent subcellular localisations in the cell ranging from the early secretory pathway (ER: SPP and SPPL2c; Golgi: SPPL3) to the plasma membrane (SPPL2b) and endosomal/lysosomal compartments (SPPL2a) [2]. In order

Abbreviations

Atp5e, ATP synthase F1 subunit epsilon; BMDC, bone marrow-derived dendritic cells; BMDM, bone marrow-derived macrophages; GAPDH, glyceraldehyde 3-phosphate dehydrogenase; GM-CSF, granulocyte-macrophage colony-stimulating factor; HpT, hypoxanthine-guanine phosphoribosyltransferase; NTF, N-terminal fragment; SNARE, soluble *N*-ethylmaleimide-sensitive factor attachment protein receptor; SPP, signal-peptide peptidase; SPPL, signal-peptide peptidase like; Stx, syntaxin; TA, tail-anchored; Tbp, TATA-Box-binding protein; VAMP, vesicle-associated membrane protein.

to be cleaved by SPP/SPPL proteases, substrate proteins need to exhibit a type II transmembrane topology characterised by a cytosolic N terminus [1,2]. Beyond this prerequisite, substrate requirements differ within this protease family. This refers mainly to the tolerated size of the substrate's ectodomain or luminal domain respectively. Whereas SPPL3 when cleaving glycosyltransferases [3,4] does not have restrictions with regard to a substrate's ectodomain size [5], the other family members fail to cleave substrates with ectodomains longer than ~60 amino acids [6]. Although certain exceptions to this rule were reported for SPP [7] and recently also for SPPL2a [8], in most other cases, processing by SPP or SPPL2a-c depends on a short ectodomain/luminal domain. This is the reason why the action of these proteases is often embedded in a proteolytic chain of events usually referred to as regulated intramembrane proteolysis [9], where first the ectodomain of a type II transmembrane protein is shortened by another protease and then the remaining membrane-bound N-terminal fragment (NTF) is subjected to intramembrane cleavage by the SPP/SPPL protease.

The finding that selected ER-localised tail-anchored (TA) proteins are processed by SPP [10–12] identified this membrane protein class as a new group of potential SPP/SPPL substrates. TA proteins exhibit a type II-oriented transmembrane segment close to the C terminus, so that the N terminus and most of the protein face the cytosol, whereas usually only very few C-terminal residues are exposed to the organelle lumen or the extracellular space respectively. Typically, membrane insertion of these proteins occurs post-translationally [13–15]. Beyond SPP, SPPL2c has also been found to cleave several TA proteins upon overexpression [16,17]. Of these, phospholamban and syntaxin-8 (Stx8) have been validated *in vivo* based on an accumulation in the testis of SPPL2c-deficient mice.

Importantly, SPP and SPPL2c cleave only selected TA proteins, and their known substrate spectra overlap only partially even under overexpression conditions. This points to specific mechanisms of substrate selection which are currently unknown. Cleavage of TA proteins by SPPL2a or SPPL2b has not been reported yet. So far, all known substrates are NTFs proteolytically derived from type II transmembrane proteins [1,2]. As more than 400 human TA proteins were predicted [18], it seems conceivable that some of these may be substrates of SPPL2a/b.

Stx18 and Stx8, which are cleaved by SPP [12] or SPPL2c [16,17], belong to the family of SNARE (soluble *N*-ethylmaleimide-sensitive factor attachment protein receptor) proteins [19]. Although initially and

most extensively characterised in the context of synaptic vesicle exocytosis [20], SNARE proteins drive most cellular membrane fusion events along the secretory pathway and in the endosomal/lysosomal system [21]. Therefore, the functional roles of individual SNARE proteins vary according to their subcellular localisation, possibly also depending on the cell type. In general, different SNARE proteins on the donor and target membrane form complexes of four-helical coiled-coil bundles that bring the two membranes in close proximity [21]. While most of the 38 known human SNAREs are TA proteins, 7 do not exhibit a transmembrane domain [21]. SNARE proteins can be classified as R and Q-SNAREs based on critical arginine and glutamine residues. One R-SNARE and three Q-SNAREs form a SNARE complex. After facilitating membrane fusion, SNARE complexes can be disassembled, for which the ATPase *N*-ethylmaleimide-sensitive factor (NSF) and the NSF attachment proteins α or γ (α -SNAP, γ -SNAP) are required [21,22], and the individual SNAREs can participate in another cycle of membrane fusion. This recycling, however, requires SNARE protein recovery from the target back to the donor membrane as illustrated by endocytosis of synaptic SNARE proteins to reform synaptic vesicles [23].

Despite their critical role, very little is known about how cellular levels of SNARE proteins are controlled and where and how these proteins are degraded. Given that levels of certain syntaxins in the ER are regulated by SPP and SPPL2c [12,16,17], we considered that SPPL2a or SPPL2b may be involved in mediating the turnover of certain SNARE proteins in the compartments where the proteases reside. Here, we screened a broad spectrum of SNARE proteins with a documented role in the late secretory or endocytic pathway for cleavage by SPPL2a and SPPL2b. In cellular substrate–protease co-expression assays, we identified VAMP1–4 as substrates of these proteases. We confirmed the relevance of this finding by demonstrating the accumulation of these R-SNAREs in several tissues and cell types of SPPL2a/b-deficient mice.

Results

None of the analysed Q-SNARE proteins are proteolysed by SPPL2a/b

Since the Q-SNARE proteins Stx8 and Stx18 had been identified as substrates of the ER-resident intramembrane proteases SPPL2c and SPP [12,17], respectively, we wanted to investigate if the homologous proteases SPPL2a and SPPL2b may also be involved in

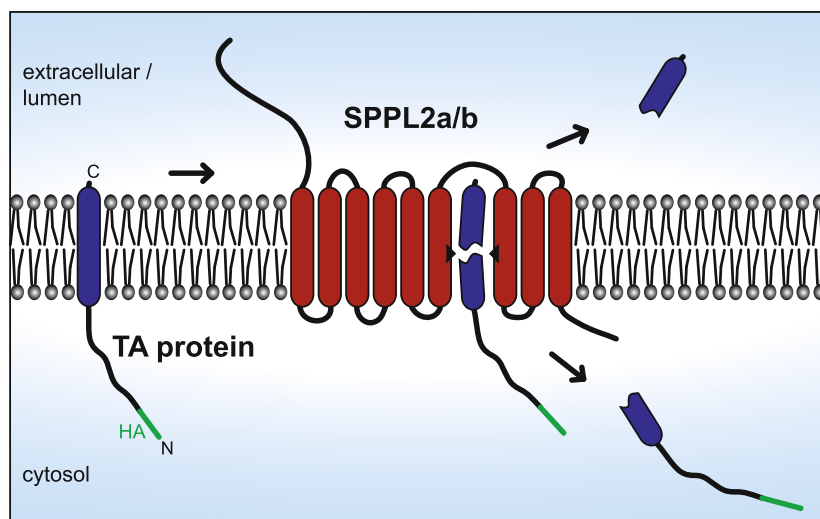


Fig. 1. Cleavage of tail-anchored proteins by SPP/SPPL intramembrane proteases. Tail-anchored (TA) proteins exhibit a cytosolic N-terminus and are anchored to the membrane with a transmembrane domain very close to their C terminus. Therefore, they can be cleaved by SPPL2 proteases directly. In the protease-substrate co-expression assays performed in this study, the analysed SNARE proteins were expressed with an HA epitope fused to their N-terminus to facilitate detection.

regulating SNARE proteins. Based on the reported predominant subcellular localisations of the two proteases in the endosomal/lysosomal system or at the plasma membrane, respectively, we selected 18 different candidate SNARE proteins (some including different isoforms) with a documented role in the late secretory and endocytic pathways. Only proteins with a TA topology, thus a single-transmembrane domain in type II orientation, were included. Due to the lack of an *in vitro* assay of SPPL2a/b with purified components, we made use of co-expression assays in HeLa cells in order to test for the cleavage of candidate substrates.

As illustrated in Fig. 1, intramembrane cleavage of TA proteins by SPP/SPPL proteases is assumed to occur directly without the need for any preceding processing by a shedding protease and releases cleavage products to either side of the membrane. In the co-expression assay, an HA epitope was fused to the N terminus of the murine SNARE proteins. Thus, detection with anti-HA should in principle visualise both, the uncleaved substrate as well as any potential cytosolic cleavage fragment. To test for intramembrane proteolysis, we co-expressed the HA-tagged SNAREs with murine SPPL2a or SPPL2b. As a control for non-proteolytic events, proteolytically inactive protease constructs were included where critical aspartates in the active centres have been replaced by alanines (SPPL2a-D416A and SPPL2b-D414A). Expression of the proteases was confirmed by western blotting. According to the scheme, cleavage of a TA protein by an SPP/SPPL protease should reduce steady-state levels of the substrate protein, which would thus be expected in samples with co-expression of the active enzymes and which also in previous studies has been

the primary readout for cleavage in such assays [10,12,16,17]. In addition, bands representing cleavage fragments may appear.

Based on two syntaxins being SPP/SPPL2c substrates, we initially tested syntaxins and other Q-SNARE substrate candidates for processing by SPPL2a/b. Cleavage assays of Stx1a, Stx1b, Stx2, Stx3, Stx4, Stx6, Stx7, Stx12, Stx16, Vti1a (vesicle transport through interaction with t-SNAREs homologue 1A), Vti1b (vesicle transport through interaction with t-SNAREs homologue 1B), GOSR1 (Golgi SNAP receptor complex member 1) and an additional isoform of Stx3 (not shown) are depicted in Fig. 2A–L. In this candidate screen, none of the analysed Q-SNAREs was modulated by SPPL2a or SPPL2b. Therefore, we conclude that the screened Q-SNAREs are not processed by SPPL2a and SPPL2b under these conditions.

Selected R-SNARE proteins are cleaved by SPPL2a/b upon overexpression

We went on to analyse different R-SNAREs belonging to the vesicle-associated membrane protein (VAMP) family in the described assay set-up. In cells expressing VAMP1 (Synaptobrevin-1), wild-type SPPL2a or SPPL2b clearly led to a reduction in VAMP1. This was seen irrespective of whether the VAMP1a (Fig. 3A) or VAMP1b (Fig. 3B) isoform was expressed. Importantly, catalytically inactive SPPL2a or SPPL2b did not lead to the depletion of VAMP1. These results indicated proteolytic processing of VAMP1 by both SPPL2a and SPPL2b in the cell-based assay. Similar results were obtained for VAMP2 (Synaptobrevin-2; Fig. 3C), VAMP3 (Cellubrevin;

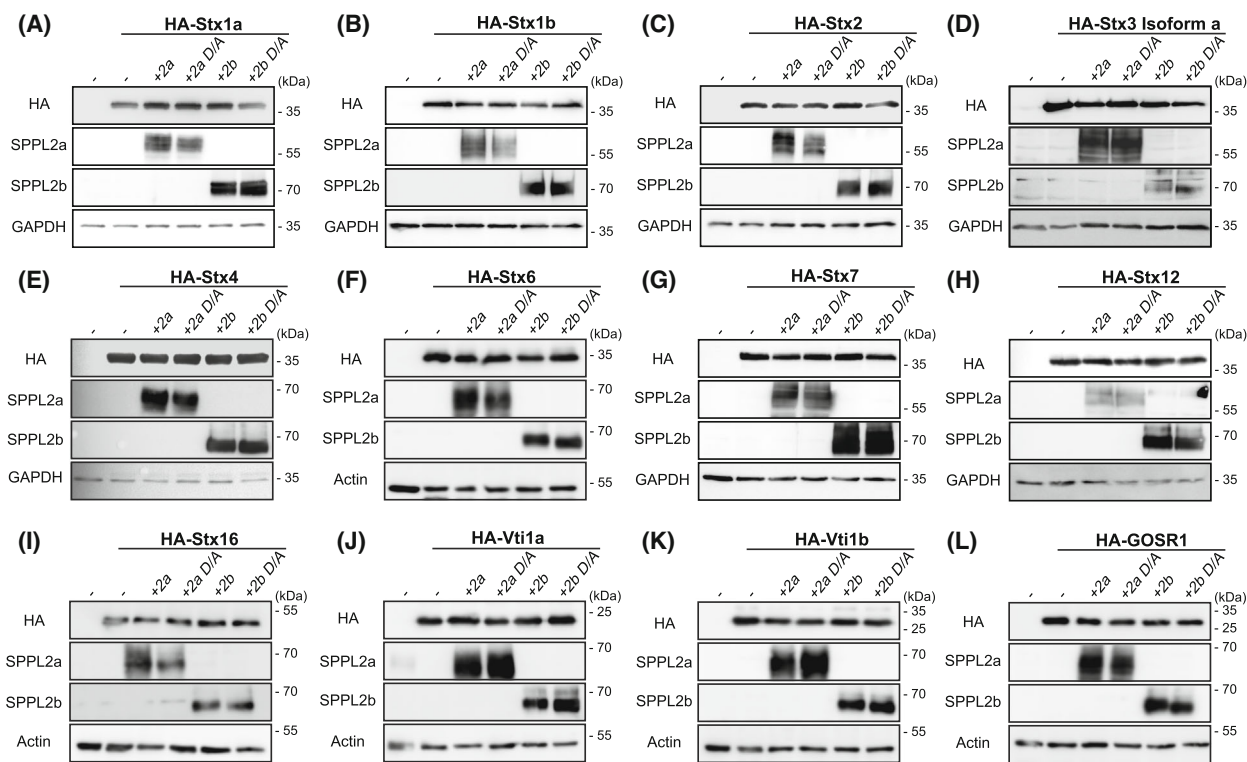


Fig. 2. Screening of selected Q-SNAREs for cleavage by the intramembrane proteases SPPL2a/b. HeLa cells were transiently transfected with expression constructs encoding the following murine SNARE proteins fused to an N-terminal HA epitope: Stx1a (A), Stx1b (B), Stx2 (C), Stx3 isoform a (D), Stx4 (E), Stx6 (F), Stx7 (G), Stx12 (H), Stx16 (I), Vti1a (J), Vti1b (K) and GOSR1 (L). Proteolytic cleavage by murine SPPL2a (2a) or SPPL2b (2b) was assessed by co-expressing the active proteases or their inactive mutants (D/A) as indicated. Upon western blotting, the expressed SNARE proteins were visualised by anti-HA, whereas antisera specifically detecting murine SPPL2a or SPPL2b were employed to confirm protease expression. Equal protein loading was confirmed by analysis of GAPDH or actin. The depicted western blots are representative of at least three independent experimental repetitions.

Fig. 3D) and two isoforms of VAMP4 (Fig. 3E,F), demonstrating cleavability of these proteins by SPPL2a or SPPL2b. Importantly, VAMP5 and VAMP8 (Endobrevin) appeared to be different from the other analysed R-SNAREs as they were not modulated by SPPL2a or SPPL2b under the conditions tested (Fig. 3G,H).

Despite the reduced steady-state levels of VAMP1-4, no additional bands that could represent SPPL2a/b-dependent cleavage fragments were readily observed (Fig. 3A–F). We enhanced the sensitivity of detection by significantly prolonging exposure time so that bands representing the full-length proteins were strongly overexposed. Under these conditions, we observed bands with a slightly lower molecular weight than the precursor which specifically appeared upon co-expression of active proteases in the case of VAMP1 isoform a (Fig. 3I), VAMP2 (Fig. 3J), VAMP3 (Fig. 3K) and VAMP4 isoform 1 (Fig. 3L). The low abundance of these proteolytic fragments

may indicate that they are only transiently present and rapidly subjected to further degradation. Hence, we tried to stabilise the fragments by inhibition of calpains since some SNARE proteins are cleaved by these enzymes [24,25], or inhibition of the proteasome as the major protein degradation system in the cytosol (Fig. 3I–L). However, none of these treatments increased the abundance of the VAMP1-4-derived fragments. We also created a VAMP2 mutant where all lysines were replaced by arginines (VAMP2-K/R) in order to prevent ubiquitination as the canonical proteasome-targeting signal (Fig. 3M). Removal of lysines depleted two faint bands with higher apparent molecular weights than the main VAMP2 band, therefore presumably representing ubiquitinated VAMP2. However, the K/R exchange did not increase steady-state levels of the cleavage fragments generated by SPPL2a/b. Altogether, this indicates that turnover of intracellular VAMP1-4 cleavage products occurs independently of the

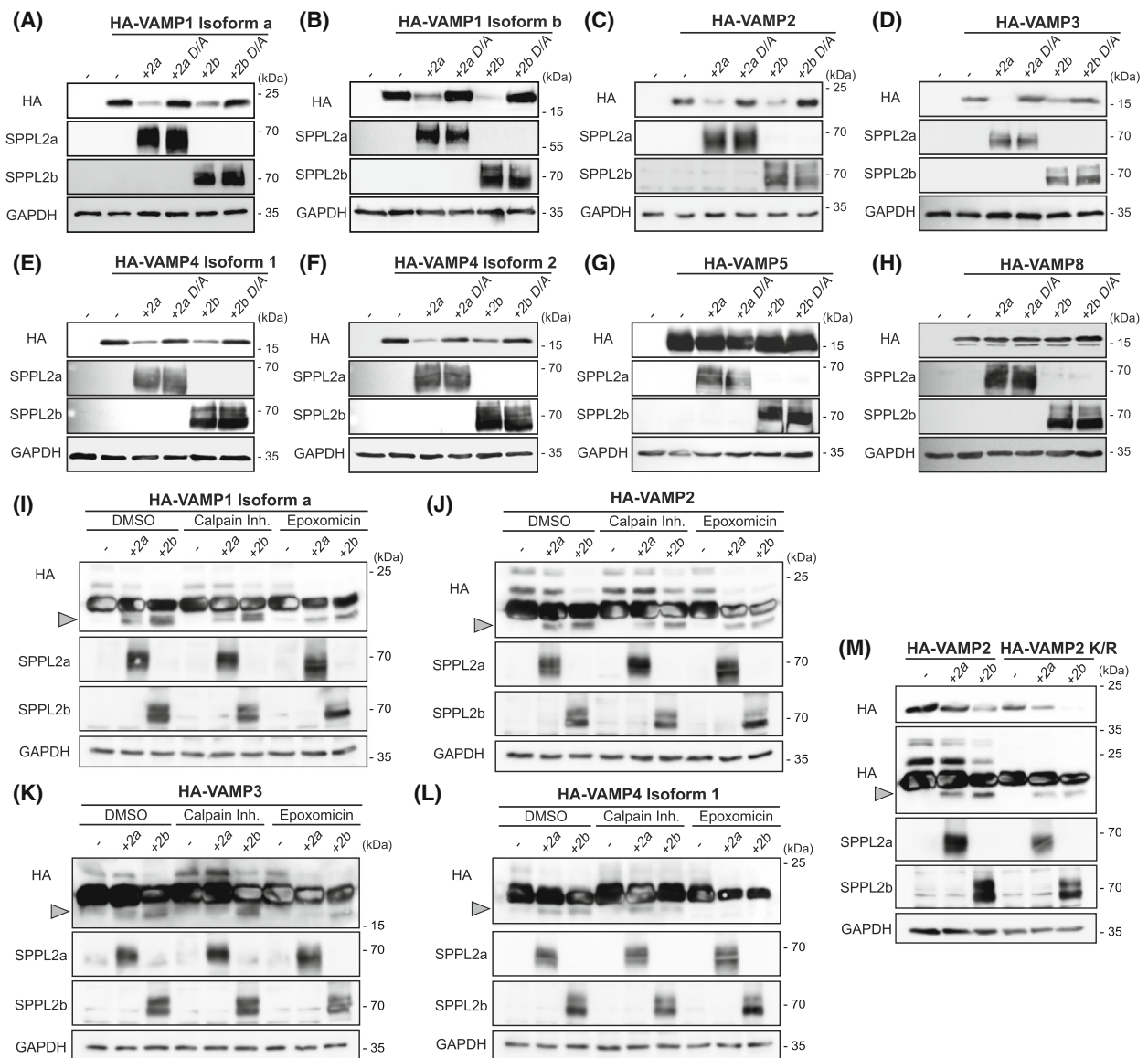


Fig. 3. Screening of selected R-SNAREs for cleavage by the intramembrane proteases SPPL2a/b. The murine R-SNAREs VAMP1 isoform a (A), VAMP1 isoform b (B), VAMP2 (C), VAMP3 (D), VAMP4 isoform 1 (Iso1) (E), VAMP4 isoform 2 (Iso2) (F), VAMP5 (G) and VAMP8 (H) were transiently expressed in HeLa cells. Where indicated, the SNARE proteins were co-expressed with active murine SPPL2a (2a) or SPPL2b (2b) or their inactive mutants (D/A). In order to analyse degradation routes of potential cleavage fragments, HeLa cells transfected with VAMP1 isoform a (I), VAMP2 (J), VAMP3 (K) or VAMP4 isoform 1 (L) and SPPL2a or SPPL2b were treated with 20 μ M calpain inhibitor III or 1 μ M epoxomicin for 16 h. Cleavage fragments generated by co-expressed SPPL2 proteases are marked with grey arrowheads. (M) Processing of a VAMP2 variant where all lysine residues have been mutated to arginine (K/R) was compared to that of wild-type VAMP2. The SNARE proteins were analysed by western blotting based on their N-terminally fused HA epitope. Expression of the proteases was confirmed with antisera specifically detecting murine SPPL2a and SPPL2b. Equal protein loading was confirmed by analysis of GAPDH. The depicted western blots are representative of at least three independent experimental repetitions.

ubiquitin–proteasome system by a yet-to-be-identified mechanism.

In conclusion, these experiments identify the R-SNAREs VAMP1–4 as potential substrates of both SPPL2a and SPPL2b. Interestingly, cleavability does not extend to the

entire family of R-SNAREs as we obtained no indication for cleavage of VAMP5 and VAMP8 similar to the analysed Q-SNAREs (Fig. 2). As just 4 different proteins of 18 SNAREs tested undergo processing by SPPL2a/b, cleavage by SPPL2a/b seems to be rather selective.

Subcellular localisation is not sufficient to explain cleavage selectivity

As substrates and proteases are membrane bound, the presence of both proteins in the same compartment will be a prerequisite for cleavage. Therefore, subcellular distributions of SNARE proteins, which were found to be cleaved by SPPL2a and SPPL2b, should at least partially overlap with the proteases in this experimental system. To demonstrate this, we co-expressed the candidate substrates with the inactive mutants of SPPL2a and SPPL2b, thereby preventing any potential bias due to proteolysis (Fig. 4). VAMP1a (Fig. 4A, isoform b not shown), VAMP2 (Fig. 4B), VAMP3 (Fig. 4C) and VAMP4 isoform 1 (Fig. 4D, isoform 2 not shown) were detected to varying degrees at the plasma membrane or in intracellular vesicular compartments, which could be part of the secretory or endocytic pathway. The extent of co-localisation with either protease varied. However, at least a partial co-localisation was seen in all cases supporting the described proteolysis.

We considered that a lack of co-localisation could also be a reason why other SNARE proteins were not proteolysed by SPPL2a/b. Therefore, we performed a similar immunocytochemical analysis for all other candidate substrates (Fig. 4E–P, Stx1b and VAMP5 not shown). In the case of GOSR1, which was detected in a Golgi-like distribution (Fig. 4E), its residence in a different compartment than the two proteases may indeed explain the lack of proteolysis. However, in many cases, distributions of SNAREs and proteases were strongly overlapping. In others, the degree of co-localisation was subtler but still detectable. This excludes that missing cleavage of the majority of candidate SNAREs can be explained by a failure to encounter the proteases in this assay and, instead, points to an intrinsic non-cleavability of these proteins.

The size of the extra-membranous domains influences the cleavability of VAMP2/4

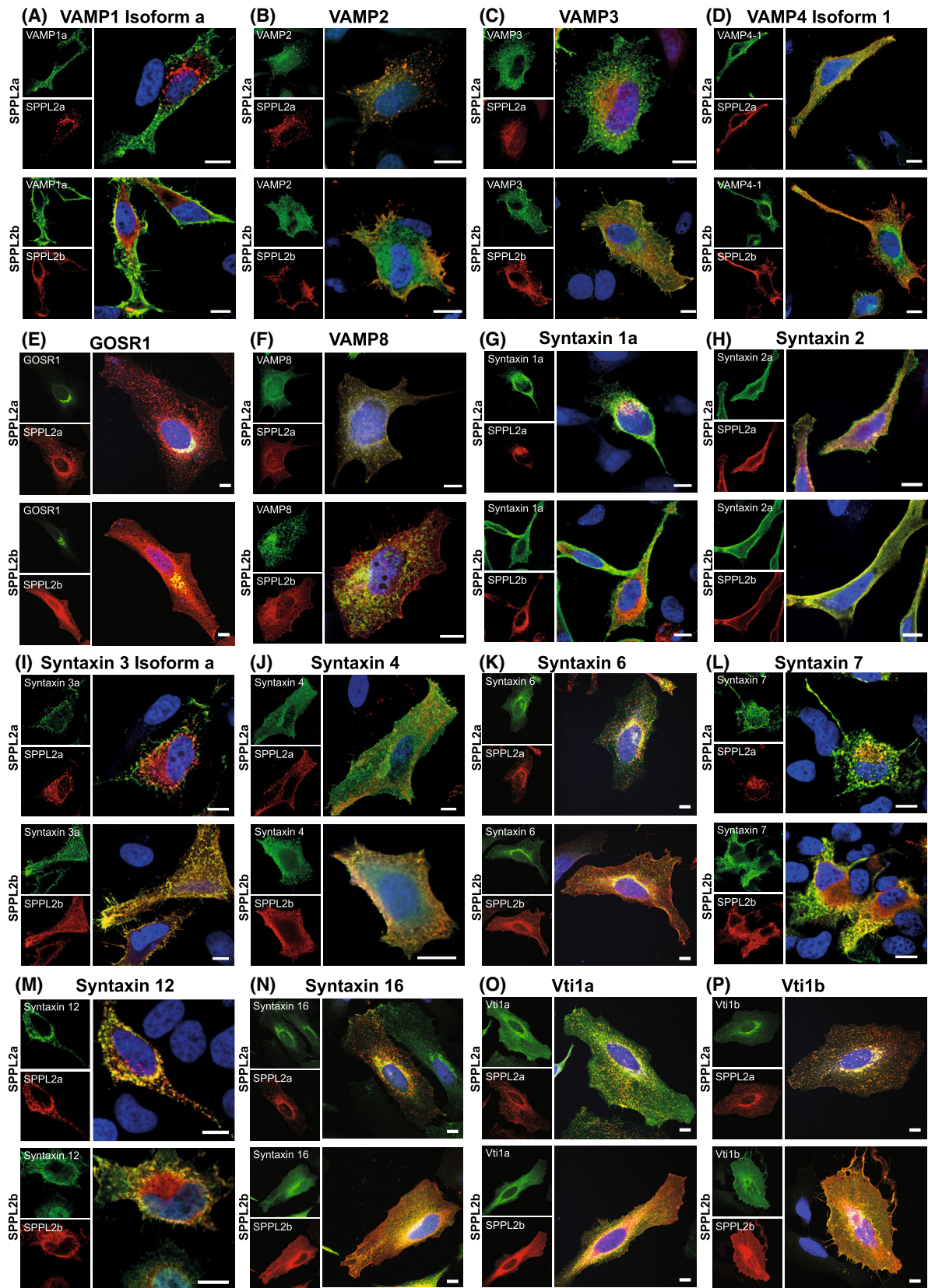
An obvious difference between the cleaved VAMP1-4 and the analysed R-SNAREs, of which none was

cleaved, is the size of the cytosolic domains, which is ~2-fold longer in the latter. We considered this as a potential determinant of cleavability. Therefore, we tested how the fusion of GFP to the N-terminus of VAMP2 or VAMP4 would influence processing by SPPL2a/b (Fig. 5A). As it was previously reported, SPPL2 proteases do not tolerate large luminal/ecto-domains [6], we also generated C-terminal GFP fusion proteins (Fig. 5A) to test this concept in the context of tail-anchored proteins. Neither the GFP-VAMP2/4 (Fig. 5B) nor the VAMP2/4-GFP (Fig. 5C) fusion proteins were processed by co-expressed SPPL2a/b. VAMP4-GFP (Fig. 5D) showed a Golgi-like distribution in line with previous studies [26], where its steady-state overlap with the proteases was limited under these conditions, which could explain the lack of processing. In contrast, GFP-VAMP4 (Fig. 5E) was very prominently co-localised with SPPL2a in vesicular compartments, whereas VAMP2-GFP (Fig. 5F) and GFP-VAMP2 (Fig. 5G) overlapped significantly with SPPL2b at the cell surface and partially also with SPPL2a in intracellular compartments. In conclusion, this indicates that increasing the size of the extra-membranous domains of VAMP2 and VAMP4 by GFP is not compatible with proteolysis by SPPL2a/b.

Inhibition of SPPL2a/b stabilises endogenous VAMP1-4

We consider the cell-based cleavage assay as a means to determine the general cleavability of candidate substrates. Thus, not all substrates identified by this approach may be relevant in a physiological context. For that reason, we wanted to assess if cleavage of the substrate candidates VAMP1-4 by SPPL2a or SPPL2b also occurs when only endogenous levels of proteases and putative substrates are present. We treated HeLa cells with the SPP/SPPL inhibitor (Z-LL)₂-ketone-targeting SPPL2a/b [27] (Fig. 6A) and quantified the abundance of the endogenous VAMP2, VAMP3 and VAMP4 proteins by western blotting, while we were unable to detect VAMP1. VAMP2 was significantly enriched by the inhibitor treatment. However, levels of VAMP3 and VAMP4 were not affected. Thus,

Fig. 4. Co-localisation of selected SNARE proteins with the intramembrane proteases SPPL2a/b. HeLa cells co-expressing the SNARE proteins VAMP1 isoform a (A), VAMP2 (B), VAMP3 (C), VAMP4 isoform 1 (D), GOSR1 (E), VAMP8 (F), Syntaxin 1a (G), Syntaxin 2 (H), Syntaxin 3 isoform a (I), Syntaxin 4 (J), Syntaxin 6 (K), Syntaxin 7 (L), Syntaxin 12 (M), Syntaxin 16 (N), Vti1a (O) or Vti1b (P) fused to an N-terminal HA epitope and the inactive murine protease mutants SPPL2a-D416A (SPPL2a) or SPPL2b-D414A (SPPL2b), both fused to a C-terminal Myc epitope, were analysed by indirect immunofluorescence. The subcellular distribution of the potential SNARE substrate and the proteases was assessed following immunocytochemical stainings using anti-HA and anti-Myc, respectively, in combination with fluorophore-conjugated secondary antibodies. Scale bar, 10 μ m. Data are representative of at least three independent experiments.



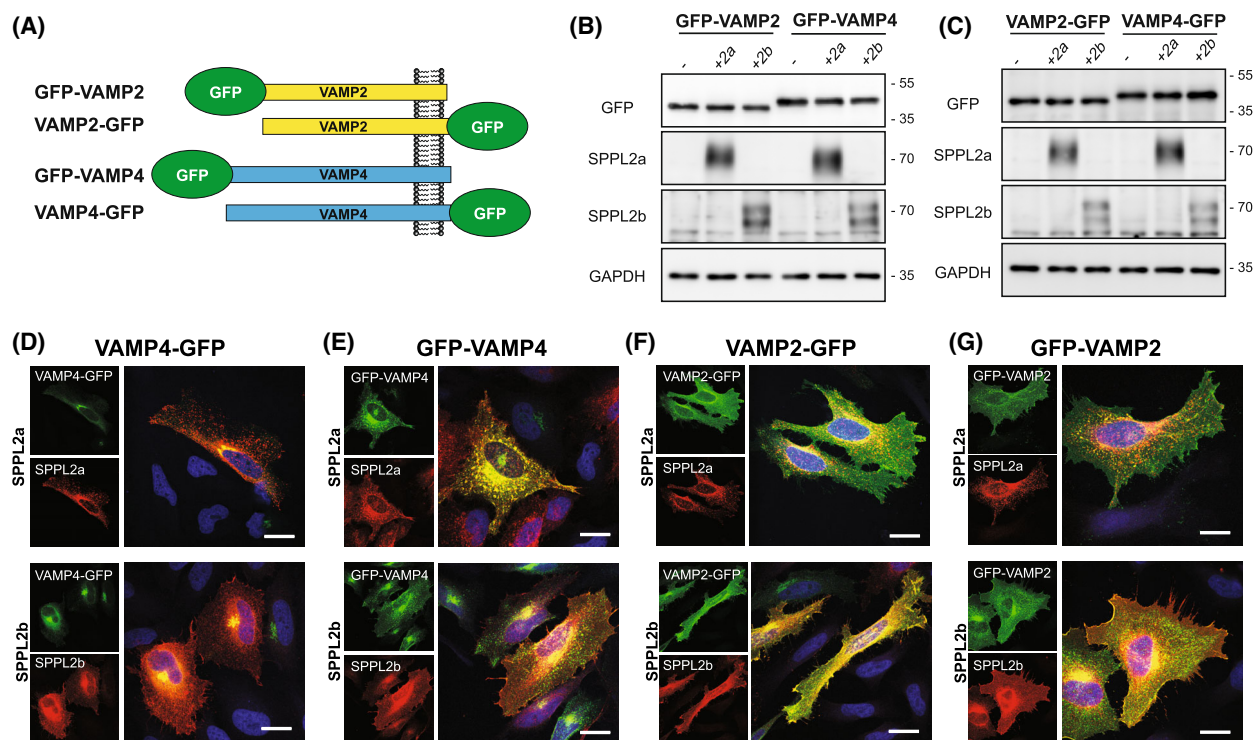


Fig. 5. The size of the extramembranous domains influences intramembrane cleavage of SNARE proteins by SPPL2a/b. (A) Scheme of GFP fusion proteins, which were generated for murine VAMP2 and VAMP4 isoform 1. (B, C) Fusion proteins of VAMP2 or VAMP4 carrying GFP at the N terminus (B, GFP-VAMP2, GFP-VAMP4) or the C terminus (C, VAMP2-GFP and VAMP4-GFP) were analysed for proteolysis by co-expressed SPPL2a or SPPL2b in HeLa cells. The SNARE-GFP fusion proteins were detected with anti-GFP. Expression of the proteases was confirmed with antisera specifically detecting murine SPPL2a and SPPL2b. Equal protein loading was confirmed by analysis of GAPDH. (D–G) Subcellular distributions of VAMP4-GFP (D), GFP-VAMP4 (E), VAMP2-GFP (F) or GFP-VAMP2 (G) were visualised following transient co-transfection with SPPL2a-D416A or SPPL2b-D414A fused to a C-terminal Myc epitope by indirect immunofluorescence. Immunocytochemical stainings were performed using anti-Myc in combination with a fluorophore-conjugated secondary antibody in order to visualise the protease. Scale bar, 20 μ m. Data are representative of at least three independent experiments.

altogether effects were rather subtle. We repeated the experiment in N2a neuroblastoma cells based on the specific role of SNARE proteins in neuronal cells (Fig. 6B). Here, VAMP1 could be quantified and was found to be significantly stabilised upon SPPL2a/b inhibition, which was also seen for VAMP2 and VAMP3. However, no major changes in VAMP4 levels were observed. In summary, these effects corroborate that VAMP1, VAMP2 and VAMP3 are substrates of SPPL2a/b. However, the role of these proteases in the turnover of these SNAREs seems to vary between different cell types, at least in the case of VAMP3.

SPPL2a/b mediates turnover of VAMP1-4 *in vivo* in a cell type and tissue-dependent manner

Due to the unfavourable properties of (Z-LL)₂-ketone, pharmacological inhibition of SPPL2a/b with this compound is often incomplete [2,27]. Therefore, we

analysed the homeostasis of the respective four SNARE proteins in SPPL2a/b double-deficient (dKO) mice [28] with constitutive and complete deficiency of both proteases (Figs 7 and 8). Based on the results from the N2a cells and the well-established function of SNAREs in neurotransmission, we initially compared the abundance of VAMP1-4 in total lysates of brains from wild-type and SPPL2a/b-deficient mice (Fig. 7A). We observed tendencies for an increase in VAMP4 in the latter. Protein levels of VAMP1 and VAMP3 were significantly but only subtly increased in the brains of the protease-deficient mice, whereas VAMP2 was unaffected. These results only partly recapitulated the findings from the inhibitor-treated neuroblastoma cells (Fig. 6B). Obviously, in addition to neurons, the brain is composed of many other different cell types and its regions differ significantly in architecture and composition. The cerebellum seems to exhibit a higher proportion of neurons in relation to glia cells than other brain parts [29]. Thus, we specifically selected this part

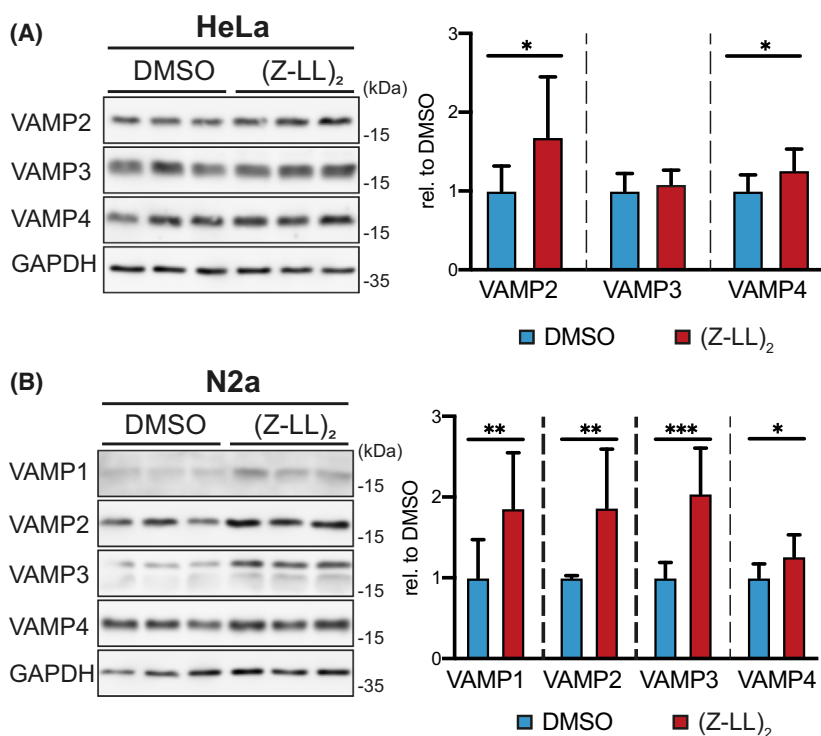


Fig. 6. Inhibition of SPPL2 proteases stabilises selected R-SNAREs in a cell-type-dependent way. HeLa (A) or N2A (B) cells were treated with 40 μM (Z-LL)₂-ketone for 24 h in order to inhibit the activity of SPPL2a/b. DMSO-treated cells were analysed as a control. Endogenous levels of VAMP1 (B) and VAMP2-4 (A, B) were determined by western blotting and quantified densitometrically. GAPDH levels were analysed to confirm equal protein loading. VAMP protein levels normalised to GAPDH and the mean of the respective DMSO-treated samples is shown as means \pm SD from $N = 3$ independent experiments with $n = 8$ (N2A-DMSO) or $n = 9$ replicates (all other). An unpaired, two-tailed Student's *t*-test was performed. * $P < 0.05$; ** $P < 0.01$; *** $P < 0.001$.

for further analysis (Fig. 7B). Here, the accumulation of VAMP4 was corroborated this time in a statistically significant manner. Similar to VAMP4, levels of VAMP1 and VAMP3 were significantly increased in dKO cerebella, in a range ~ 1.5 – 2 fold. Again, no effect was seen on VAMP2. As a control, we compared the mRNA expression of VAMP1-4 in the cerebella of both genotypes (Fig. 7C), which were similar. In the absence of differences in gene expression, the accumulation of VAMP1, VAMP3 and VAMP4 very likely is caused post-translationally, which is in line with the role of the intramembrane proteases in the turnover of these SNARE proteins. Altogether, our data validate these SNARE proteins as *in vivo* substrates of SPPL2a/b. However, as these effects were less pronounced in the total brain, processing by the intramembrane proteases may occur in a cell-type-dependent way.

Beyond their role in synapses, SNARE proteins facilitate membrane fusion in the secretory and endocytic pathways of many other cell types. Consequently, many of them are widely expressed. Hence, we analysed levels of VAMP1-4 in additional tissues of dKO mice. We failed to detect VAMP1 in non-neural tissues. However, we were able to quantify VAMP2, VAMP3 and VAMP4 protein levels in the heart (Fig. 8A), pancreas (Fig. 8B), liver (Fig. 8C), spleen (Fig. 8D), thymus (Fig. 8E), bone marrow-derived dendritic cells (Fig. 8F) and macrophages (Fig. 8G). A

clear accumulation of VAMP2 and VAMP4 was observed in all analysed tissues or primary immune cell types from SPPL2a/b-deficient mice. In contrast, the effects of protease ablation on VAMP3 homeostasis differed. A significant increase was seen in the heart, pancreas and thymus but not in the liver, dendritic cells, macrophages and spleen. We aimed to exclude that the observed increased steady-state SNARE levels were caused by alternative mechanisms leading to enhanced transcription of *Vamp2*, *Vamp3* and *Vamp4*. With the exception of a minor upregulation of *Vamp2* mRNA levels in the liver of *SPPL2a/b*^{-/-} mice (Fig. 8H), mRNA levels of *Vamp2-4* were unaffected in the liver (Fig. 8H) and heart (Fig. 8I) of these mice. In macrophages (Fig. 8J) and dendritic cells (Fig. 8K), we even observed a significant downregulation of *Vamp2* and *Vamp4* mRNA levels, which could represent a compensatory mechanism for the accumulation of the respective proteins. Taken together, these results demonstrate that the increased steady-state levels of VAMP2, VAMP3 and VAMP4 proteins upon loss of SPPL2a/b are indeed caused by a post-translational mechanism. This result is consistent with a reduced turnover in absence of proteolysis by SPPL2a/b. In conclusion, we confirmed all four VAMP proteins identified in the overexpression screening approach as substrates of SPPL2a/b. However, the extent of cleavage varies significantly between different cell types and tissues.

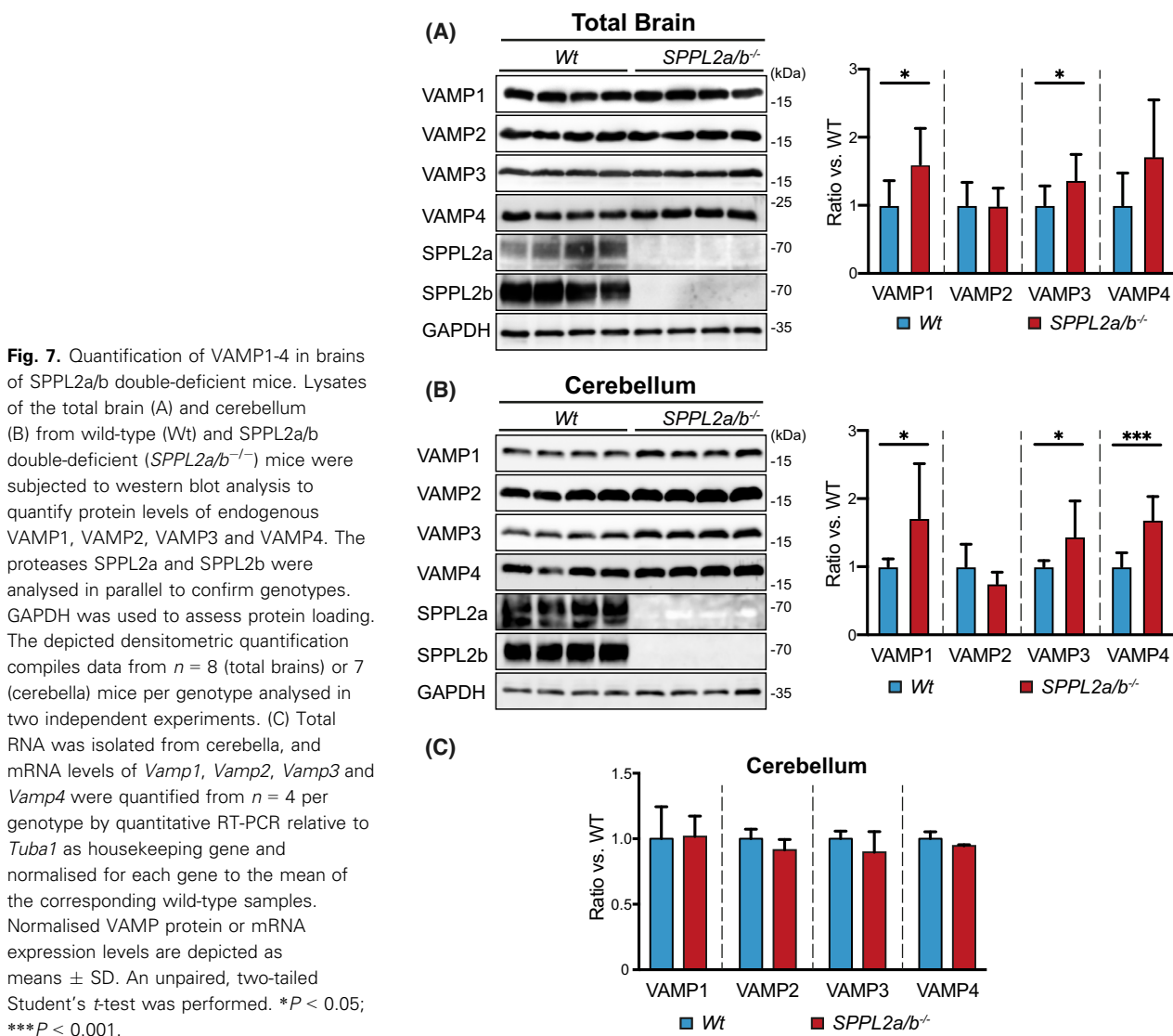


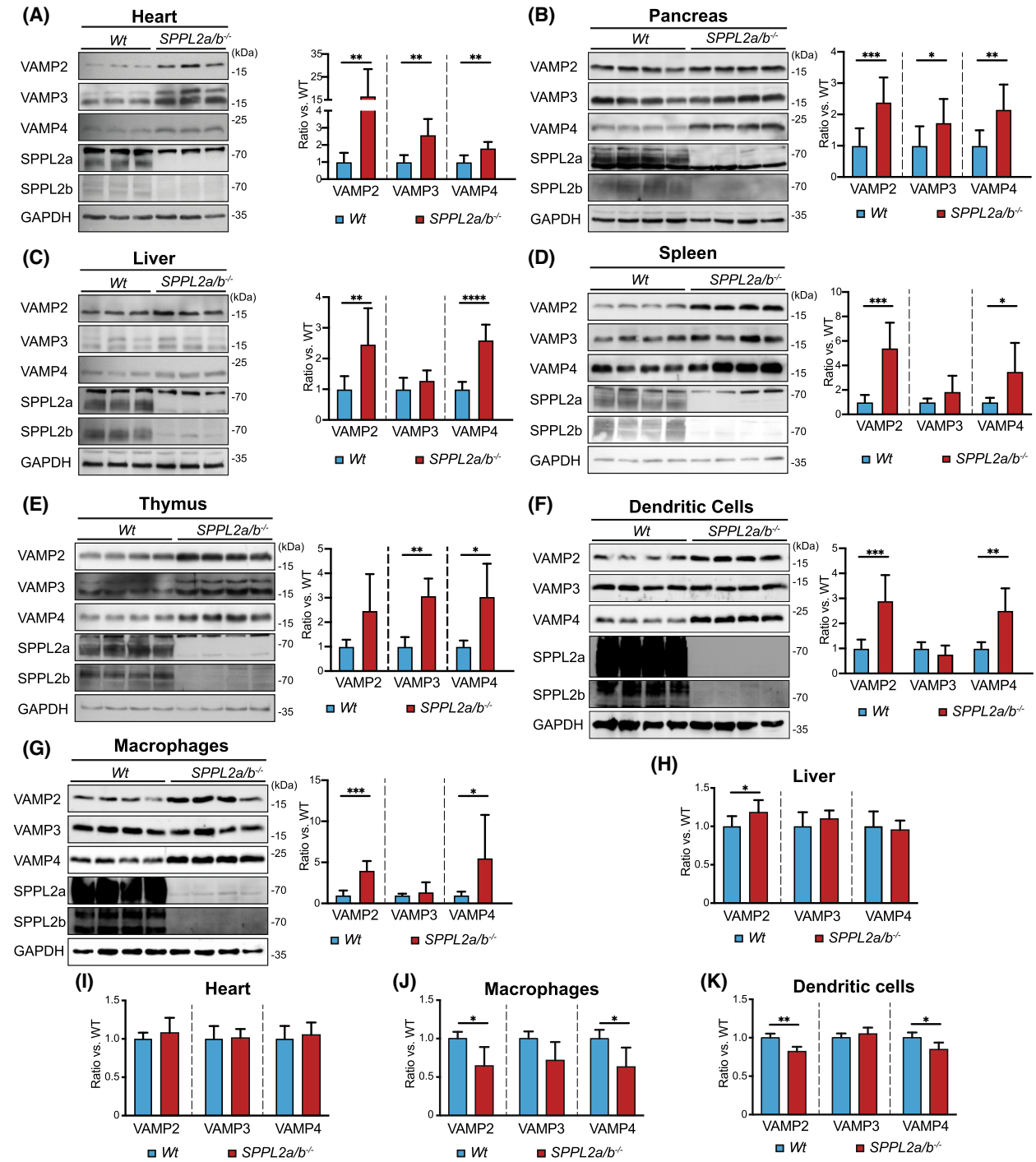
Fig. 7. Quantification of VAMP1-4 in brains of SPPL2a/b double-deficient mice. Lysates of the total brain (A) and cerebellum (B) from wild-type (Wt) and SPPL2a/b double-deficient (*SPPL2a/b*^{-/-}) mice were subjected to western blot analysis to quantify protein levels of endogenous VAMP1, VAMP2, VAMP3 and VAMP4. The proteases SPPL2a and SPPL2b were analysed in parallel to confirm genotypes. GAPDH was used to assess protein loading. The depicted densitometric quantification compiles data from *n* = 8 (total brains) or 7 (cerebella) mice per genotype analysed in two independent experiments. (C) Total RNA was isolated from cerebella, and mRNA levels of *Vamp1*, *Vamp2*, *Vamp3* and *Vamp4* were quantified from *n* = 4 per genotype by quantitative RT-PCR relative to *Tuba1* as housekeeping gene and normalised for each gene to the mean of the corresponding wild-type samples. Normalised VAMP protein or mRNA expression levels are depicted as means ± SD. An unpaired, two-tailed Student's *t*-test was performed. **P* < 0.05; ****P* < 0.001.

Discussion

Our data *in vivo* validate the SNARE proteins VAMP1-4 as validated substrates of the intramembrane proteases SPPL2a and SPPL2b. This

demonstrates that the capability to cleave TA proteins within the SPP/SPPL family is not limited to SPP [10–12] and SPPL2c [16,17] and significantly broadens the potential substrate spectrum of SPPL2a/b. Our results

Fig. 8. Accumulation of VAMP2-4 in several non-neural tissues or cell types of *SPPL2a/b*^{-/-} mice. Total lysates of the heart (A), pancreas (B), liver (C), spleen (D), thymus (E), bone marrow-derived dendritic cells (F) and bone marrow-derived macrophages (G) from wild-type (Wt) and SPPL2a/b double-deficient (*SPPL2a/b*^{-/-}) were analysed by western blotting. Endogenous VAMP2, VAMP3 and VAMP4 levels were compared and quantified densitometrically. The absence of SPPL2a and SPPL2b in samples from *SPPL2a/b*^{-/-} mice confirmed the genotypes. GAPDH was detected to demonstrate equal protein loading. The depicted quantifications summarise data from *n* = 4 (thymus), 6 (heart), 7 (liver, spleen and dendritic cells) or 10 (pancreas and macrophages) mice per genotype, which were analysed in one (thymus), two (heart, liver, spleen and dendritic cells) or three (pancreas and macrophages) independent experiments. Normalised VAMP protein levels are shown as means ± SD. (H, I) Total RNA was isolated from the liver (H), heart (I), bone marrow-derived macrophages (J) or bone marrow-derived dendritic cells (K) and mRNA levels of *Vamp2*, *Vamp3* and *Vamp4* were quantified by quantitative RT-PCR relative to the mean of three housekeeping genes, *Atp5e*, *Hprt* and *Tbp* (H) or to *Tuba1* as housekeeping gene (I–K), and were normalised for each gene to the mean of the wild-type samples. Means ± SD from *n* = 4 (dendritic cells and macrophages), 5 (heart) or 8 (liver) are depicted. An unpaired, two-tailed Student's *t*-test was performed. **P* < 0.05; ***P* < 0.01; ****P* < 0.001.



advocate also examination of TA proteins [18] other than SNAREs as putative substrates of intramembrane proteolysis. Furthermore, our findings extend the concept of naturally short substrates of intramembrane proteases which also applies to γ -secretase-mediated cleavage [30]. However, of the 18 SNARE proteins

and additional isoforms assessed for potential proteolysis by SPPL2a/b, only VAMP1-4 were found to be cleaved in the initial SNARE-protease co-expression screen. Despite its localisation in late endosomes and lysosomes [21], VAMP7 is missing in this analysis as we failed to achieve sufficient expression levels using

HA-tagged expression constructs. Cleavage of TA proteins by SPPL2a/b seems to be highly selective, which is in line with previous findings for SPP and SPPL2c [1]. Apparently, TA topology and co-localisation with the protease within the same subcellular compartment are required but not sufficient preconditions for cleavage. Instead, additional features seem to be involved in determining that VAMP1-4 are substrates of SPPL2a/b, whereas none of the analysed syntaxins was cleaved in our hands. This is surprising, as certain syntaxins have been identified as substrates of SPP and SPPL2c [12,17]. It is currently unclear, which features determine the cleavability of VAMP1-4 versus other SNAREs. Certain flexibility of the substrate's transmembrane domain which usually correlates with the presence of helix-destabilising amino acids like proline and glycine seems to support cleavage by SPP/SPPL proteases and other intramembrane proteases in general [1,31]. With regard to the mere presence of such residues, there does not seem to be an obvious difference between transmembrane segments of SNAREs identified as SPPL2a/b substrates or non-substrates in this study. Therefore, it is also possible that the differential cleavability of SNAREs by SPPL2a/b is rather determined by properties of the cytosolic domains, which are larger in the syntaxins. This hypothesis may be supported by our results from the GFP fusion proteins (Fig. 5), which indicate that a large cytosolic domain prevents cleavage by SPPL2a/b. However, VAMP5 and VAMP8, which exhibit a similar size cytosolic domain as VAMP1-4, were not processed in our hands, which may point to more specific requirements in addition to size.

The observed accumulation of VAMP1-4 in different tissues of SPPL2a/b-deficient mice clearly demonstrates that cleavage of these substrates occurs in a physiological system – although with varying impact in different tissues. SNARE proteins may be assumed to be accessible for proteolytic cleavage only in their free form, but not when being part of a SNARE complex [22]. Under endogenous conditions, the ratio between both forms may determine the extent of processing taking place. Whereas total VAMP2 and VAMP4 were robustly increased in all peripheral non-neural dKO tissues analysed, the accumulation of VAMP3 was more variable and only observed in some tissues. Even more strikingly, in the brain, the homeostasis of VAMP1-4 was only very subtly affected strongly contrasting the other organs. In addition to neurons, the CNS also contains different types of glia cells [29]. VAMP proteins are present and exhibit important functions also in astrocytes [32–35] and oligodendrocytes [36–38], which may also be anticipated for

macrophage-like microglia actively performing exocytosis and phagocytosis [39]. Nothing is known so far about the distribution of SPPL2a within the brain. Based on a β -galactosidase reporter, expression of SPPL2b seemed to be quite prominent in neurons [28]. However, this has not been confirmed at the protein level and it is unclear in which parts of the neurons SPPL2b is present. This information would be important as VAMP2 and VAMP4 in addition to their well-documented role in synaptic vesicle exocytosis have also been localised to dendrites [40], where they are involved in the sorting of post-synaptic receptors. The results from total brain indeed indicate that at least in some cerebral cell types, SPPL2a/b do not relevantly contribute to VAMP1-4 turnover. However, it can only be speculated to what extent the different cell types contribute to the overall detected proteins. In cerebellum, VAMP1, VAMP3 and VAMP4 are significantly accumulated in the absence of SPPL2a/b. Interestingly, the cerebellum was noted to exhibit a lower glia/neuron ratio than other parts of the brain [29] so neurons should have a higher contribution to the overall protein composition here.

An open question is the molecular function of the cleavage of VAMP1-4 by SPPL2a/b. In general, cytosolic cleavage fragments liberated by intramembrane proteases can fulfil biological functions [41,42]. However, VAMP1-4-derived cleavage fragments were detected only at very low levels even under overexpression conditions, which is in line with many other SPP/SPPL substrates [1,10]. Soluble domains of SNARE proteins devoid of their transmembrane domain were shown to inhibit membrane fusion in a dominant-negative way by forming non-functional complexes with other membrane-bound SNARE proteins [43,44]. Hence, a build-up of VAMP1-4 cleavage products in the cytosol may be problematic making a rapid turnover necessary. How this is achieved remains to be clarified. Our results indicate that calpains and the ubiquitin–proteasome system do not play a major role in this.

We propose that the primary task of SPPL2a/b is to control cellular levels of the membrane-bound VAMP1-4 and to mediate their turnover. Despite long-standing work on SNARE proteins, surprisingly little is known about how these proteins are degraded by cells. In the case of syntaxin1, degradation by the proteasome following ubiquitination was observed [45]. In neurons, the turnover of VAMP2 [46] and VAMP4 [47] was found to be accelerated by cellular/synaptic activity. When directly comparing the half-life of these proteins in activated pre-synapses upon fusion with fluorescent timer proteins, VAMP4 exhibited a

more rapid turnover than VAMP2 and was particularly short lived due to delivery to endo-lysosomal compartments [47]. How VAMP4 is degraded there currently remains an open question. Being a trans-membrane protein mostly facing the cytosol, just delivering it to the limiting membrane of lysosomes by itself would not expose it to lysosomal proteases sequestered within this organelle. To solve this topological problem, one would need to postulate sorting into intraluminal vesicles, e.g. by the endosomal sorting complex required for transport (ESCRT) pathway [48]. Indeed, activity-dependent degradation of VAMP2 relied on the ESCRT machinery [46]. Whether this sorting is initiated by ubiquitination remains to be addressed. Ubiquitination of VAMP3 by a specific E3 ligase has been observed [49], but its relevance for the turnover of the protein still needs to be determined. Thus, there are many open questions about how the degradation of SNARE proteins is achieved mechanistically. Intramembrane proteolysis of VAMP1-4 by SPPL2a/b has to be added to the emerging picture. Cleaving these proteins directly in the plane of cellular membranes circumvents the need for ESCRT sorting or any hypothetical pathway to extract the protein from the membrane for degradation by the proteasome. Based on our results regarding VAMP2/4 fused to GFP, it needs to be considered that the fusion proteins of VAMP1-4 with large fluorescent tags are likely to behave differently from the wild-type proteins in terms of protein homeostasis and stability, as this appears to exclude them from SPPL2a/b-mediated turnover.

Having concluded that the intramembrane cleavage of VAMP1-4 may be primarily a degradative event, the question remains if this occurs in a constitutive, homeostatic way or is rather a triggered, regulated event. Currently, there is not much known about the regulation of SPPL2a/b proteases [1]. Anyway, it remains to be proven that the degree of VAMP modulation achieved by SPPL2a/b has a relevant impact on trafficking. However, in mice carrying a specific point mutation in the *Vamp2* gene, VAMP2 protein levels were reduced by about 30%, which was linked with altered synaptic function, behavioural deficits and disturbance of sleep [50]. Similarly, also increased levels of VAMP4 in synapses, which can be induced by blocking lysosomal degradation of VAMP4, led to reduced synaptic vesicle release probability [47]. These examples indicate that modulation of SNARE levels can affect membrane trafficking and even lead to phenotypic consequences in neurons *in vivo*. Importantly, VAMP2-4 are broadly expressed in the body supporting exocytotic events in many different cell types

[21,51] including immune cells [39], pancreatic beta cells [52], adipocytes [53], myotubes [54] and spermatozoa [55,56]. Altogether, this advocates investigating different mechanisms of SNARE homeostasis including the intramembrane proteases SPPL2a and SPPL2b in a broader way.

Materials and methods

Experimental animals

Mice with a knockout of both SPPL2a and SPPL2b have been described and characterised previously [28]. All analysed mice were on a C57BL/6N *Cr1* background with age- and sex-matched wild-type animals serving as controls. Breeding and sacrificing of mice have been approved by the Ministerium für Energiewende, Landwirtschaft, Umwelt und ländliche Räume of Schleswig-Holstein (V 242.7224.121-3) or the Landesdirektion Sachsen (TV A 12/2018, DD24.1-5131/450/12) respectively. Animal care and handling were performed in accordance with local and national guidelines. Mice were housed in individually ventilated cages in the animal facilities of the Christian-Albrechts-University Kiel or within the Medizinisch-Theoretisches Zentrum, TU Dresden.

Plasmids

Plasmids encoding wild-type murine SPPL2a and SPPL2b fused to a C-terminal Myc tag as well as their catalytically inactive mutants SPPL2a D416A and SPPL2b D414A were described before [28,57,58]. Expression constructs of the SNARE proteins were generated by amplifying the open reading frame of the desired protein from murine cDNA via PCR. The used ORFs corresponded to the following database entries: [NM_016810.4](#) (GOSR1), [NM_016801.4](#) (syntaxin-1a, STX1a); [NM_024414.2](#) (Syntaxin-1b, STX1b); [NM_007941.3](#) (Syntaxin-2, STX2); [NM_152220.2](#) (Syntaxin-3 Isoform a, STX3a); [NM_001286543.2](#) (Syntaxin-3 Isoform d, Stx3d); [NM_009294.3](#) (Syntaxin-4, STX4); [NM_021433.3](#) (Syntaxin-6, STX6); [NM_001358563.1](#) (Syntaxin-7, STX7); [NM_133887.4](#) (Syntaxin-12, STX12); [NM_172675.4](#) (Syntaxin-16, STX16); [NM_009496.3](#) (VAMP1a); [NM_001080557.1](#) (VAMP1b); [NM_009497.3](#) (VAMP2); [NM_009498.4](#) (VAMP3); [NM_001356526.1](#) (VAMP4 Isoform 1); [NM_001347125.1](#) (VAMP4 Isoform 2); [NM_001080742.2](#) (VAMP5); [NM_016794.3](#) (VAMP8); [NM_016862.4](#) (Vti1a); and [NM_016800.3](#) (Vti1b). Using extended primers, an N-terminal HA epitope tag was appended to the 5' end of the respective open reading frames upon amplification and all PCR products were inserted into pcDNA3.1 Hygro(+). With the exception of VAMP4 and STX12, which were cloned via *BamHI* and *XhoI* restriction sites, and STX7 ORF, which was inserted

via *HindIII* and *NotI* restriction sites, all other inserts were integrated using *HindIII* and *XhoI* restriction sites. In order to express C- or N-terminal GFP fusion proteins of murine VAMP2 and VAMP4 isoform 1, the respective open reading frames were inserted into peGFP-N1 using *XhoI* and *BamHI* restriction sites or peGFP-C1 via *BglII* and *EcoRI* sites so that coding sequences of the SNARE proteins and GFP were in-frame. All obtained constructs were verified by sequencing (GATC, Konstanz, Germany; SeqLab, Göttingen, Germany).

Cell lines and cell culture

HeLa (DSMZ, Braunschweig, Germany) and NEURO-2a (N2A) cells (DSMZ) were cultivated in DMEM (GIBCO, Paisley, UK) supplemented with 10% FCS (Biochrom, Berlin, Germany; Thermo Fisher, Waltham, MA, USA), 100 U·mL⁻¹ penicillin (Sigma, Taufkirchen, Germany) and 100 µg·mL⁻¹ streptomycin (Sigma). Generation and cultivation of bone marrow-derived dendritic cells and bone marrow-derived macrophages are described below. Cells were maintained at 37 °C with a humidified 5% CO₂/95% air atmosphere. As indicated in the figure legends, (Z-LL)₂-ketone (Peptanova, Sandhausen, Germany) was applied at a final concentration of 40 µM to inhibit substrate processing by SPPL proteases. For inhibition of the proteasome or calpain proteases, epoxomicin (Peptanova) or calpain inhibitor III (Cayman Chemical, Ann Arbor, MI, USA) were used at final concentrations of 1 or 20 µM respectively. Transfection of cells (1 µg DNA per well) was conducted using Turbofect (Thermo) or polyethylenimine (PEI). One day prior to transfection, cells were seeded onto six-well plates. After 5–6 h, the medium was changed and the cells were either harvested for western blot analysis or fixed for immunocytochemical staining on a subsequent day.

Generation of murine bone marrow-derived immune cells

Bone marrow-derived macrophages (BMDM) and bone marrow-derived dendritic cells (BMDC) were differentiated from murine bone marrow as described before [28,59,60]. Red bone marrow was obtained from the tibia and femur and single-cell suspensions were prepared as described in the following depending on the desired cell type. To generate BMDC, 5 × 10⁶ cells were seeded in 10 cm Petri dishes (Sarstedt, Nümbrecht, Germany) in 10 mL of the BMDC medium (RPMI 1640 + 10% (v/v) FCS + 50 mM β-mercaptoethanol + 100 U·mL⁻¹ penicillin + 100 µg·mL⁻¹ streptomycin) supplemented with 20 ng·mL⁻¹ recombinant murine granulocyte-macrophage colony-stimulating factor (GM-CSF, Immunotools, Friesoythe, Germany). After 3 days, 10 mL BMDC medium with 20 ng·mL⁻¹ GM-CSF was added. Six days after seeding, 10 mL of the medium was exchanged for 10 mL of fresh medium containing

10 ng·mL⁻¹ rmGM-CSF. The cells were harvested 8 days after isolation from the bone marrow for analysis. BMDM were differentiated using a total amount of 10⁷ cells cultured in 10 mL BMDM medium (DMEM +20% (v/v) FCS + 100 U·mL⁻¹ penicillin + 100 µg·mL⁻¹ streptomycin) supplemented with 50 ng·mL⁻¹ recombinant murine macrophage colony-stimulating factor (M-CSF, Immunotools) in 10 cm petri dishes. After 3 days, 5 mL of M-CSF-supplemented BMDM medium was added. BMDM were harvested and used for experiments after 7 days of differentiation.

Protein extraction from tissues and cells

Protein was extracted from cultured cells or snap-frozen tissue. Whenever possible, samples were kept on ice or at 4 °C. Tissue homogenisation buffer (50 mM Tris-HCl, pH 7.4, 150 mM NaCl, 4 mM EDTA, 1× Complete Protease Inhibitor Cocktail (Roche, Mannheim, Germany), 4 mM Pefabloc® SC Protease Inhibitor (Carl Roth, Karlsruhe, Germany) and 0.5 mg·mL⁻¹ Pepstatin A (Sigma)) was added in a 1 : 10 ratio based on the weight of the tissue samples. In case of softer tissues (e.g. brain samples), ceramic beads were added and the sample was homogenised using a PreCelllys homogeniser for 2 × 30 s at 6500 r.p.m. More durable tissues (e.g. muscle or heart) were homogenised with a tissue blender (Ultra-Turrax). After disruption, the tissue homogenates were adjusted to final concentrations of 1% (w/v) Triton X-100 and 0.1% (w/v) SDS, incubated on ice for 1 h and sonicated twice during that time (20 pulses at 4 °C, level 4, Branson Sonifier 450, Emerson Industrial Automation). Subsequently, debris (and ceramic beads) were cleared from the lysate by centrifugation (10 min at 17 000 × g) and the supernatant was transferred to a fresh tube.

To extract protein from cultured cells, adherent cells were washed with cold PBS and scraped off in PBS Complete (1× PBS, pH 7.4, 1× Complete Protease Inhibitor Cocktail (Roche), 4 mM EDTA). BMDC were harvested and washed in PBS as described [59] so that adherent and suspension cells were combined for the analysis. In all cases, cell suspensions were finally centrifuged for 10 min at 900 × g and the supernatant was discarded. The cell pellets were resuspended in 50–100 µL lysis buffer (50 mM Tris-HCl, pH 7.4, 150 mM NaCl, 1% (w/v) Triton X-100, 0.1% (w/v) SDS and 4 mM EDTA, plus protease inhibitors as in tissue homogenisation buffer). The resuspended cells were mechanically disrupted by pipetting and sonication (20 pulses, level 4) and incubated on ice for 1 h. Afterwards, lysates were cleared by centrifugation as described above. Protein concentration of tissue and cell lysates was determined using Pierce™ Bicinchoninic Acid (BCA) Protein Assay Kit (Thermo Fisher) following the manufacturer's recommendations in a 96-well plate format using a bovine serum albumin (BSA) standard curve ranging from 0 to 2 mg·mL⁻¹. The remaining lysate was adjusted to final

concentrations of 1% (w/v) SDS, 100 mM dithiothreitol, 125 mM Tris-HCl, pH 6.8 and 10% (v/v) glycerol in preparation for western blot analysis.

SDS/PAGE and western blot analysis

Proteins extracted from cell and tissue samples were separated by SDS/PAGE with a buffer system according to Laemmli [61]. Depending on the molecular weight of the proteins of interest, gels with total acrylamide concentrations of 10% or 12.5% were used. For the detection of SNARE proteins, proteins were denatured for 5 min at 95 °C, whereas for detection of SPPL proteases, samples were incubated for 10 min at 55 °C prior to electrophoresis. Aliquots of 20–50 µg protein were analysed. Following electrophoresis, proteins were transferred to nitrocellulose membranes (Whatman® Protran® nitrocellulose membrane, 0.2 µm pore size) using a semi-dry transfer protocol for 2 h as described [62]. Following transfer, the membranes were incubated in blocking buffer (5% (w/v) milk powder in TBS-T (25 mM Tris-HCl, pH 7.4, 137 mM NaCl, 2.7 mM KCl and 0.1% (v/v) Tween-20)). Overexpressed SNARE proteins were detected via the appended HA epitope using the rat monoclonal 3F10 antibody from Roche. In some experiments, a 3F10 antibody directly coupled to horseradish peroxidase (HRP) was employed. For the detection of GFP fusion proteins, rabbit monoclonal D5.1 antibody (Cell Signalling, Danvers, MA, USA) was utilised. Polyclonal antibodies against murine SPPL2a [57] and SPPL2b [28] have been described before. Endogenous SNARE proteins in murine tissues were analysed with the following primary antibodies: polyclonal anti-VAMP1 (13151, Cell Signalling), monoclonal anti-VAMP2 (Clone D6O1A, Cell Signalling), polyclonal anti-VAMP3 (GTX55838, GeneTex, Irvine, CA, USA) and polyclonal anti-VAMP4 (136002, Synaptic systems, Göttingen, Germany). To confirm equal protein loading, anti-GAPDH (sc-25778, Santa Cruz antibodies, Dallas, Texas, USA; 607901, BioLegend, San Diego, CA, USA) or anti-actin (A2066, Sigma) was employed. All primary and secondary antibodies were applied in the blocking buffer. HRP-coupled secondary antibodies were purchased from Dianova (Hamburg, Germany). In between and prior to detection, membranes were washed three times with TBS-T. Chemoluminescent visualisation of HRP activity was performed using an Amersham Imager 600 or Azure 600 imager. Images were processed with Adobe Photoshop or GIMP. Densitometric quantification of band intensities was conducted using the IMAGEJ software [63]. To facilitate a second detection round, bound antibodies were removed from a membrane either by incubation in glycine buffer (100 mM glycine, pH 2.2, 50 mM KCl and 20 mM magnesium acetate) for 30 min at room temperature or in SDS buffer (62.5 mM Tris-HCl, pH 6.8, 2% (w/v) SDS and 0.82% (v/v) β-mercaptoethanol) for 20 min at 80 °C. Subsequently,

membranes were washed and incubated in a blocking buffer before applying a new primary antibody.

Indirect immunofluorescence

Cells were seeded on glass coverslips, transfected as described above and finally, fixed with 4% (w/v) paraformaldehyde in PBS. Immunocytochemical stainings were conducted according to a previously described protocol [62]. Overexpressed SNARE proteins and SPPL2 proteases were detected based on their appended HA and Myc epitopes, respectively, using rat anti-HA (3F10, Roche) and mouse anti-Myc (9B11, Cell Signalling) as primary antibodies. For visualisation, Alexa 488- and 594-conjugated secondary antibodies (Molecular Probes, Eugene, Oregon, USA) were employed. DAPI (4',6-diamidino-2-phenylindole, Sigma) was added to the embedding medium at a concentration of 1 µg·mL⁻¹ to stain the nuclei. Specimens were analysed and images were acquired with Olympus FV1000 or Leica SP5 confocal laser scanning microscopes. Images were further processed with OLYMPUS FLUOVIEW, IMAGE J and ADOBE PHOTOSHOP software.

Quantitative RT-PCR

Total RNA was extracted from tissues or cells using TRIzol (Sigma) according to the manufacturer's instructions. Reverse transcription was performed using the RevertAid First Strand cDNA Synthesis kit (Thermo Scientific) and random hexamer oligonucleotides from 1 µg total RNA according to the manufacturer's recommendations. Gene expression of *Vamp1*, *Vamp2*, *Vamp3* and *Vamp4* in heart, BMDC, BMDM and cerebellum was analysed using the Universal Probe Library System (Roche) with a LightCycler 480 Instrument II (Roche). The following primers and hydrolysis probes were used: VAMP1 (probe #78): fw, 5'-ACGGACCTCCACTTCC TCTT-3'; rv, 5'-CAGCTCCTTCTGTCCCTTCA-3'; VAMP2 (probe #31): fw, 5'-CCAAGCTCAAGCGCAAAT-3'; rv, 5'-GGGATTTAAGTGCTGAAGTAAACG-3'; VAMP3 (probe #31): fw, 5'-TCGCAGTTTGAAACAAGTGC-3'; rv, 5'-ATCCCTATCGCCACATCTT-3'; VAMP4 (both isoforms, probe #42): fw, 5'-TGCAAGAGAATATTACAAAGGT AATTG-3'; rv, 5'-GAAAGCGGTGGCATTATCC-3'; Tubulin1a (probe #88): fw, 5'-CTGGAACCCACGGTCATC-3'; rv, 5'-GTGGCCACGAGCATAGTTATT-3'.

RNA expression analysis in liver tissue samples was carried out using the Maxima SYBR Green/ROX qPCR Master Mix (2×; Thermo Scientific) following the manufacturer's instructions. Samples were measured in a 10 µL format on a C1000 Touch™ Thermal Cycler (BioRad, Hercules, CA, USA). Expression of genes of interest was calculated relative to the mean of three housekeeping genes, *Atp5e*, *Hprt* and *Thp*, and taking primer efficiencies into account. The following primer pairs were used: VAMP2: fw, 5'-ACTGGTGGAAAAACCTCAAGATGA-

3'; rv, 5'-AGGGAGGGGGCTGAAAGATA-3'; VAMP3: fw, 5'-GAAGACTCCAGCAGACACAAA-3'; rv, 5'-CCGAGAGCTTCTGGTCTCTT-3'; VAMP4: fw, 5'-ATGATGATGACGTGACCGGG-3'; rv, 5'-TCCAGATGGTCCCCGTAGAA-3'; Atp5e: fw, 5'-CCGGTTTGAGGCTACTCTGA-3'; rv, 5'-GGAAAACCGGATGTAGCTGAGT-3'; Hprt: fw, 5'-AGTCCCAGCGTCGTGATTAG-3'; rv, 5'-TGATGGCCTCCCATCTCCTT-3'; Tbp: fw, 5'-GGCATCAGATGTGCGTCAG-3'; rv, 5'-ATGAAATAGTGATGTGGCA-3'.

Acknowledgements

We thank Sebastian Held and Petra Peche for excellent technical assistance and organisational support. Acquisition of some microscopic images was performed within the Core Facility Cellular Imaging of TU Dresden. This work was supported by the Deutsche Forschungsgemeinschaft to BSchr (125440785/SFB877, project B7; 251390220/SCHR1284/1-1, SCHR1284/1-2; and 380321491/SCHR1284/2-1), to BSchw (380321491/SCHW 823/4-1) and to TM (431664610/ME 5459/1-1). Open Access funding enabled and organized by ProjektDEAL. Open Access funding enabled and organized by Projekt DEAL.

Conflict of interest

The authors declare no conflict of interest.

Author contributions

MB, WG, MP, MK, JR-M and BF performed the experiments and analysed data. TM supervised and instructed experiments. BSchr and BSchw designed, conceptualised and supervised the research and analysed data. BSchr, MB and WG wrote the manuscript. All authors contributed to the editing of the manuscript.

Peer review

The peer review history for this article is available at <https://publons.com/publon/10.1111/febs.16610>.

Data availability statement

All data supporting the findings of this study are available within the manuscript.

References

- Mentrup T, Schröder B. Signal peptide peptidase-like 2 proteases: regulatory switches or proteasome of the

membrane? *Biochim Biophys Acta Mol Cell Res.* 2022;**1869**:119163.

- Mentrup T, Cabrera-Cabrera F, Fluhrer R, Schröder B. Physiological functions of SPP/SPPL intramembrane proteases. *Cell Mol Life Sci.* 2020;**77**:2959–79.
- Voss M, Kunzel U, Higel F, Kuhn PH, Colombo A, Fukumori A, et al. Shedding of glycan-modifying enzymes by signal peptide peptidase-like 3 (SPPL3) regulates cellular N-glycosylation. *EMBO J.* 2014;**33**:2890–905.
- Kuhn PH, Voss M, Haug-Kroper M, Schröder B, Schepers U, Brase S, et al. Secretome analysis identifies novel signal peptide peptidase-like 3 (Sppl3) substrates and reveals a role of Sppl3 in multiple Golgi glycosylation pathways. *Mol Cell Proteomics.* 2015;**14**:1584–98.
- Voss M, Fukumori A, Kuhn PH, Kunzel U, Klier B, Grammer G, et al. Foamy virus envelope protein is a substrate for signal peptide peptidase-like 3 (SPPL3). *J Biol Chem.* 2012;**287**:43401–9.
- Martin L, Fluhrer R, Haass C. Substrate requirements for SPPL2b-dependent regulated intramembrane proteolysis. *J Biol Chem.* 2009;**284**:5662–70.
- Chen CY, Malchus NS, Hehn B, Stelzer W, Avci D, Langosch D, et al. Signal peptide peptidase functions in ERAD to cleave the unfolded protein response regulator XBP1u. *EMBO J.* 2014;**33**:2492–506.
- Spitz C, Schlosser C, Guschtschin-Schmidt N, Stelzer W, Menig S, Gotz A, et al. Non-canonical shedding of TNFalpha by SPPL2a is determined by the conformational flexibility of its transmembrane helix. *iScience.* 2020;**23**:101775.
- Lichtenthaler SF, Lemberg MK, Fluhrer R. Proteolytic ectodomain shedding of membrane proteins in mammals—hardware, concepts, and recent developments. *EMBO J.* 2018;**37**:e99456.
- Boname JM, Bloor S, Wandel MP, Nathan JA, Antrobus R, Dingwell KS, et al. Cleavage by signal peptide peptidase is required for the degradation of selected tail-anchored proteins. *J Cell Biol.* 2014;**205**:847–62.
- Hsu FF, Yeh CT, Sun YJ, Chiang MT, Lan WM, Li FA, et al. Signal peptide peptidase-mediated nuclear localization of heme oxygenase-1 promotes cancer cell proliferation and invasion independent of its enzymatic activity. *Oncogene.* 2015;**34**:2360–70.
- Avci D, Malchus NS, Heidasch R, Lorenz H, Richter K, Nessling M, et al. The intramembrane protease SPP impacts morphology of the endoplasmic reticulum by triggering degradation of morphogenic proteins. *J Biol Chem.* 2019;**294**:2786–800.
- Rabu C, Schmid V, Schwappach B, High S. Biogenesis of tail-anchored proteins: the beginning for the end? *J Cell Sci.* 2009;**122**:3605–12.
- Schuldiner M, Metz J, Schmid V, Denic V, Rakwalska M, Schmitt HD, et al. The GET complex mediates

- insertion of tail-anchored proteins into the ER membrane. *Cell*. 2008;**134**:634–45.
- 15 Farkas A, Bohnsack KE. Capture and delivery of tail-anchored proteins to the endoplasmic reticulum. *J Cell Biol*. 2021;**220**:e202105004.
 - 16 Niemeyer J, Mentrup T, Heidasch R, Muller SA, Biswas U, Meyer R, et al. The intramembrane protease SPPL2c promotes male germ cell development by cleaving phospholamban. *EMBO Rep*. 2019;**20**:e46449.
 - 17 Papadopoulou AA, Muller SA, Mentrup T, Shmueli MD, Niemeyer J, Haug-Kroper M, et al. Signal peptide peptidase-like 2c (SPPL2c) impairs vesicular transport and cleavage of SNARE proteins. *EMBO Rep*. 2019;**20**:e46451.
 - 18 Kalbfleisch T, Cambon A, Wattenberg BW. A bioinformatics approach to identifying tail-anchored proteins in the human genome. *Traffic*. 2007;**8**:1687–94.
 - 19 Wang T, Li L, Hong W. SNARE proteins in membrane trafficking. *Traffic*. 2017;**18**:767–75.
 - 20 Sudhof TC. Neurotransmitter release: the last millisecond in the life of a synaptic vesicle. *Neuron*. 2013;**80**:675–90.
 - 21 Dingjan I, Linders PTA, Verboogen DRJ, Revelo NH, Ter Beest M, van den Bogaart G. Endosomal and Phagosomal SNAREs. *Physiol Rev*. 2018;**98**:1465–92.
 - 22 Bombardier JP, Munson M. Three steps forward, two steps back: mechanistic insights into the assembly and disassembly of the SNARE complex. *Curr Opin Chem Biol*. 2015;**29**:66–71.
 - 23 Sankaranarayanan S, Ryan TA. Real-time measurements of vesicle-SNARE recycling in synapses of the central nervous system. *Nat Cell Biol*. 2000;**2**:197–204.
 - 24 Rutledge TW, Whiteheart SW. SNAP-23 is a target for calpain cleavage in activated platelets. *J Biol Chem*. 2002;**277**:37009–15.
 - 25 Zimmerman UJ, Malek SK, Liu L, Li HL. Proteolysis of synaptobrevin, syntaxin, and SNAP-25 in alveolar epithelial type II cells. *IUBMB Life*. 1999;**48**:453–8.
 - 26 Tran TH, Zeng Q, Hong W. VAMP4 cycles from the cell surface to the trans-Golgi network via sorting and recycling endosomes. *J Cell Sci*. 2007;**120**:1028–41.
 - 27 Mentrup T, Loock AC, Fluhrer R, Schröder B. Signal peptide peptidase and SPP-like proteases – possible therapeutic targets? *Biochim Biophys Acta*. 2017;**1864**:2169–82.
 - 28 Schneppenheim J, Hüttl S, Mentrup T, Lüllmann-Rauch R, Rothaug M, Engelke M, et al. The intramembrane proteases signal peptide peptidase-like 2a and 2b have distinct functions in vivo. *Mol Cell Biol*. 2014;**34**:1398–411.
 - 29 Herculano-Houzel S. The glia/neuron ratio: how it varies uniformly across brain structures and species and what that means for brain physiology and evolution. *Glia*. 2014;**62**:1377–91.
 - 30 Laurent SA, Hoffmann FS, Kuhn PH, Cheng Q, Chu Y, Schmidt-Supprian M, et al. Gamma-secretase directly sheds the survival receptor BCMA from plasma cells. *Nat Commun*. 2015;**6**:7333.
 - 31 Langosch D, Scharnagl C, Steiner H, Lemberg MK. Understanding intramembrane proteolysis: from protein dynamics to reaction kinetics. *Trends Biochem Sci*. 2015;**40**:318–27.
 - 32 Ropert N, Jalil A, Li D. Expression and cellular function of vSNARE proteins in brain astrocytes. *Neuroscience*. 2016;**323**:76–83.
 - 33 Schwarz Y, Zhao N, Kirchhoff F, Bruns D. Astrocytes control synaptic strength by two distinct v-SNARE-dependent release pathways. *Nat Neurosci*. 2017;**20**:1529–39.
 - 34 Bezzi P, Gundersen V, Galbete JL, Seifert G, Steinhauser C, Pilati E, et al. Astrocytes contain a vesicular compartment that is competent for regulated exocytosis of glutamate. *Nat Neurosci*. 2004;**7**:613–20.
 - 35 Parpura V, Fang Y, Basarsky T, Jahn R, Haydon PG. Expression of synaptobrevin II, cellubrevin and syntaxin but not SNAP-25 in cultured astrocytes. *FEBS Lett*. 1995;**377**:489–92.
 - 36 Madison DL, Krueger WH, Cheng D, Trapp BD, Pfeiffer SE. SNARE complex proteins, including the cognate pair VAMP-2 and syntaxin-4, are expressed in cultured oligodendrocytes. *J Neurochem*. 1999;**72**:988–98.
 - 37 Feldmann A, Winterstein C, White R, Trotter J, Kramer-Albers EM. Comprehensive analysis of expression, subcellular localization, and cognate pairing of SNARE proteins in oligodendrocytes. *J Neurosci Res*. 2009;**87**:1760–72.
 - 38 Feldmann A, Amphornrat J, Schonherr M, Winterstein C, Mobius W, Ruhwedel T, et al. Transport of the major myelin proteolipid protein is directed by VAMP3 and VAMP7. *J Neurosci*. 2011;**31**:5659–72.
 - 39 Stow JL, Manderson AP, Murray RZ. SNAREing immunity: the role of SNAREs in the immune system. *Nat Rev Immunol*. 2006;**6**:919–29.
 - 40 Bakr M, Jullie D, Krapivkina J, Paget-Blanc V, Bouit L, Petersen JD, et al. The vSNAREs VAMP2 and VAMP4 control recycling and intracellular sorting of post-synaptic receptors in neuronal dendrites. *Cell Rep*. 2021;**36**:109678.
 - 41 Ye J. Transcription factors activated through RIP (regulated intramembrane proteolysis) and RAT (regulated alternative translocation). *J Biol Chem*. 2020;**295**:10271–80.
 - 42 Papadopoulou AA, Fluhrer R. Signaling functions of intramembrane aspartyl-proteases. *Front Cardiovasc Med*. 2020;**7**:591787.
 - 43 Scales SJ, Chen YA, Yoo BY, Patel SM, Doung YC, Scheller RH. SNAREs contribute to the specificity of membrane fusion. *Neuron*. 2000;**26**:457–64.

- 44 Hua Y, Scheller RH. Three SNARE complexes cooperate to mediate membrane fusion. *Proc Natl Acad Sci USA*. 2001;**98**:8065–70.
- 45 Chin LS, Vavalle JP, Li L. Staring, a novel E3 ubiquitin-protein ligase that targets syntaxin 1 for degradation. *J Biol Chem*. 2002;**277**:35071–9.
- 46 Sheehan P, Zhu M, Beskow A, Vollmer C, Waites CL. Activity-dependent degradation of synaptic vesicle proteins requires Rab35 and the ESCRT pathway. *J Neurosci*. 2016;**36**:8668–86.
- 47 Ivanova D, Dobson KL, Gajbhiye A, Davenport EC, Hacker D, Ultanir SK, et al. Control of synaptic vesicle release probability via VAMP4 targeting to endolysosomes. *Sci Adv*. 2021;**7**:eabf3873.
- 48 Babst M, Odorizzi G. The balance of protein expression and degradation: an ESCRTs point of view. *Curr Opin Cell Biol*. 2013;**25**:489–94.
- 49 Yamazaki Y, Schonherr C, Varshney GK, Dogru M, Hallberg B, Palmer RH. Goliath family E3 ligases regulate the recycling endosome pathway via VAMP3 ubiquitylation. *EMBO J*. 2013;**32**:524–37.
- 50 Banks GT, Guillaumin MCC, Heise I, Lau P, Yin M, Bourbia N, et al. Forward genetics identifies a novel sleep mutant with sleep state inertia and REM sleep deficits. *Sci Adv*. 2020;**6**:eabb3567.
- 51 Rossetto O, Gorza L, Schiavo G, Schiavo N, Scheller RH, Montecucco C. VAMP/synaptobrevin isoforms 1 and 2 are widely and differentially expressed in nonneuronal tissues. *J Cell Biol*. 1996;**132**:167–79.
- 52 Regazzi R, Wollheim CB, Lang J, Theler JM, Rossetto O, Montecucco C, et al. VAMP-2 and cellubrevin are expressed in pancreatic beta-cells and are essential for ca(2+)-but not for GTP gamma S-induced insulin secretion. *EMBO J*. 1995;**14**:2723–30.
- 53 Sadler JB, Bryant NJ, Gould GW. Characterization of VAMP isoforms in 3T3-L1 adipocytes: implications for GLUT4 trafficking. *Mol Biol Cell*. 2015;**26**:530–6.
- 54 Tajika Y, Takahashi M, Khairani AF, Ueno H, Murakami T, Yorifuji H. Vesicular transport system in myotubes: ultrastructural study and signposting with vesicle-associated membrane proteins. *Histochem Cell Biol*. 2014;**141**:441–54.
- 55 De Blas GA, Roggero CM, Tomes CN, Mayorga LS. Dynamics of SNARE assembly and disassembly during sperm acrosomal exocytosis. *PLoS Biol*. 2005;**3**:e323.
- 56 Guo X, Shen J, Xia Z, Zhang R, Zhang P, Zhao C, et al. Proteomic analysis of proteins involved in spermiogenesis in mouse. *J Proteome Res*. 2010;**9**:1246–56.
- 57 Behnke J, Schneppenheim J, Koch-Nolte F, Haag F, Saftig P, Schröder B. Signal-peptide-peptidase-like 2a (SPPL2a) is targeted to lysosomes/late endosomes by a tyrosine motif in its C-terminal tail. *FEBS Lett*. 2011;**585**:2951–7.
- 58 Schneppenheim J, Dressel R, Hüttel S, Lüllmann-Rauch R, Engelke M, Dittmann K, et al. The intramembrane protease SPPL2a promotes B cell development and controls endosomal traffic by cleavage of the invariant chain. *J Exp Med*. 2013;**210**:41–58.
- 59 Gradtke AC, Mentrup T, Lehmann CHK, Cabrera-Cabrera F, Desel C, Okakpu D, et al. Deficiency of the intramembrane protease SPPL2a alters antimycobacterial cytokine responses of dendritic cells. *J Immunol*. 2021;**206**:164–80.
- 60 Mentrup T, Stumpff-Niggemann AY, Leinung N, Schlosser C, Schubert K, Wehner R, et al. Phagosomal signalling of the C-type lectin receptor Dectin-1 is terminated by intramembrane proteolysis. *Nat Commun*. 2022;**13**:1880.
- 61 Laemmli UK. Cleavage of structural proteins during the assembly of the head of bacteriophage T4. *Nature*. 1970;**227**:680–5.
- 62 Schröder B, Wrocklage C, Hasilik A, Saftig P. Molecular characterisation of 'transmembrane protein 192' (TMEM192), a novel protein of the lysosomal membrane. *Biol Chem*. 2010;**391**:695–704.
- 63 Schneider CA, Rasband WS, Eliceiri KW. NIH Image to ImageJ: 25 years of image analysis. *Nat Methods*. 2012;**9**:671–675.